Acta Oceanol. Sin., 2021, Vol. 40, No. 5, P. 30–35
https://doi.org/10.1007/s13131-021-1726-1
http://www.hyxb.org.cn
E-mail: ocean2@hyxb.org.cn

A rapid assessment method for calculating the drag coefficient in wave attenuation by vegetation

Zhilin Zhang[1, 2, 3, 4, 6], Bensheng Huang[1, 2, 3, 4*], Hongxiang Ji[1, 2, 3, 4], Xin Tian[5], Jing Qiu[1, 2, 3, 4], Chao Tan[1, 2, 3, 4], Xiangju Cheng[6]

[1] Guangdong Research Institute of Water Resources and Hydropower, Guangzhou 510630, China

[2] State and Local Joint Engineering Laboratory of Estuarine and Hydraulic Technology, Guangzhou 510630, China

[3] Guangdong Key Laboratory of Hydrodynamic Research, Guangzhou 510630, China

[4] Technical Research Center of Guangdong-Hong Kong-Macao Greater Bay Area's Water Safety Guarantee, Guangzhou 510630, China

[5] Department of Water Management, Delft University of Technology, Delft 2628 CN, the Netherlands

[6] School of Civil Engineering and Transportation, South China University of Technology, Guangzhou 510640, China

Received 17 March 2020; accepted 11 June 2020

Abstract

Vegetation in wetlands is a large-scale nature-based resource that can provide multiple benefits to human beings and the environment, such as wave attenuation in coastal zones. Traditionally, there are two main calibration approaches to calculate the attenuation of wave driven by vegetation. The first method is a straightforward one based on the exponential attenuation of wave height in the direction of wave transmission, which, however, overlooks the crucial drag coefficient (C_D). The other method is in accordance with more complicate equations for predicting the damping factor, which is regarded as a function of C_D. In this study, a new relation, combining these above two conventional approaches, is proposed to predict the C_D in an operative approach. Results show that values yielded by the new assessment method perform a strong linear relationship with a collection of historical observations, with a promising R^2 value of 0.90. Besides, the linear regression derives a new predictive equation for the bulk drag coefficient. Additionally, a calibrated value of 4 for the empirical plant drag coefficient (C_P) is revealed. Overall, this new equation, with the superiority of the convenient exponential regression, is expected to be a rapid assessment method for calculating wave attenuation by vegetation and predicting the drag coefficient.

Key words: wave attenuation by vegetation, nature-based coast, drag coefficient, empirical validation

Citation: Zhang Zhilin, Huang Bensheng, Ji Hongxiang, Tian Xin, Qiu Jing, Tan Chao, Cheng Xiangju. 2021. A rapid assessment method for calculating the drag coefficient in wave attenuation by vegetation. Acta Oceanologica Sinica, 40(5): 30–35, doi: 10.1007/s13131-021-1726-1

1 Introduction

The estuarine and coastal area is an ecological habitat, commonly with abundant resources. This area provides water, food, energy, minerals, fishery and other resources for human beings, serving as an important place for leisure, recreation, and transportation. However, coastal areas, especially at low altitudes, have long been at risk of flooding from hurricanes and other extreme storm events, and the water security is not guaranteed; sea-level rise and climate change could also lead to increased frequency and intensity of storms, exacerbating the threat (Anderson et al., 2011). Most of the existing single seawalls are difficult to meet the current wave prevention requirements, hence, it is of practical significance to consider the natural conditions and construct the ecological safety barrier with wetland vegetation, which can enhance the toughness of the coast and save construction investment effectively (Reguero et al., 2018). Practice has proved that wetland vegetation in China (Liu et al., 2019), Vietnam (Mazda et al., 1997), Malaysia (Ghazali et al., 2016), Indonesia (Yanagisawa et al., 2010), Sri Lanka (Tanaka et al., 2007), India (Danielsen et al., 2005), Thailand (Thampanya et al., 2006) and other places have effectively protected the coast by dissipating incoming wave energy. Vegetation in wetlands as a large-scale nature-based solution can also provide services such as increasing bank stability, enhancing coastal ecosystem and biodiversity, enhancing fisheries and forestry production, and promoting tourism economy, whereas the vegetation occupies floodplain resources (Schaubroeck, 2017; Keesstra et al., 2018).

Therefore, it is necessary to understand the mechanism of wave attenuation, fueling the efficiency of the nature-based solution. It is assumed that the influence of vegetation on the flow field can be expressed by the resistance acting on the vegetation (Kobayashi et al., 1993). No matter which kind of approach is used, such as numerical modeling (Wu et al., 2016; Suzuki et al., 2019), laboratory experiment (Houser et al., 2015; Peruzzo et al.,

Foundation item: The National Key Research and Development Program of China under contract No. 2016YFC0402607; the Key Research and Development Projects in Guangdong Province under contract No. 2019B111101002; the 2018 Guangzhou Science and Technology Project under contract No. 201806010143; the Water Resource Science and Technology Innovation Program of Guangdong Province under contract No. 2017-17.

*Corresponding author, E-mail: bensheng@21cn.com

2018), or field study (Quartel et al., 2007), wave attenuation by vegetation is mainly induced by the drag force (F_D) provided by the vegetation acting on the water motion. The drag force is closely related to the drag coefficient (C_D) which is used to quantify the drag or resistance of vegetation in water. Since the drag coefficient can be quite different on different time and space scales, this parameter is one of the most uncertain parameters in the complicate interaction between vegetation and water. Parameterizing C_D was mainly by two methods, calibration or direct measurement (Chen et al., 2018). The calibration method comes from the perspective of wave energy dissipation and will be presented in detail in Section 2. The direct measurement method is based on the acting force on the vegetation, and the periodic averaged drag coefficient is obtained by calculating the work done by the drag force over one period. It is crucial to connect these two methods to reduce the uncertainties related to the drag coefficient, however, Chen et al. (2018) had considered the combined current-wave flow condition following Losada et al. (2016) which can be expanded to other cases.

This paper aims to reveal an effective method for rapidly assessing wave attenuation by vegetation following the conventional calibration approaches, and comparing the predicted value from the new method to the historical observation either by calibration method or direct measurement method. This eliminates the need for different formulas for different operating conditions and to form a unified, simplified and rapid assessment technology.

2 Calibration method to the drag coefficient

The calibration method determines the drag coefficient (C_D) from the perspective of wave energy dissipation, represented by the decay of wave height. Following one of the first hydrodynamic models for wave attenuation proposed by Dean (1979), wave height decay can be expressed as:

$$\frac{H(X)}{H_0}=\frac{1}{1+\alpha' X}, \tag{1}$$

where $H(X)$ (m) is the wave height at a distance X (m) through the vegetation field; H_0 (m) is the initial wave height measured at the start of the vegetation field; and α' (m^{-1}) is the damping factor.

Based on empirical estimates of fluid drag forces acting on vertical, rigid cylinder, Dean (1979) found that

$$\alpha'=\frac{C_D d}{6\pi h}NH_0, \tag{2}$$

where d (m) is the diameter of circular vegetation cylinder; h (m) is the water depth; and N (stems/m^2) is the average number of stems per unit area.

Then, Knutson et al. (1982) reformed Eq. (2) by incorporating an empirical plant drag coefficient, C_P, to account for the difference between rigid cylinders and plants:

$$\alpha'=\frac{C_P C_D d}{6\pi h}NH_0. \tag{3}$$

Further, Dalrymple et al. (1984) formulated an algebraic dissipation equation practicing linear wave theory and conservation of wave energy by considering a vegetation bed as an array of rigid, vertical cylinders. The time-averaged energy dissipation is the product of the drag force per unit volume and the fluid velocity due to wave motion, and instead of Eq. (2), the solution was given by:

$$\alpha'=\frac{1}{3\pi}C_D N d\left(\sinh^3 k_w l_s+3\sinh k_w l_s\right)\times \left[\frac{4k_w}{3\sinh k_w h(\sinh 2k_w h+2k_w h)}\right]H_0, \tag{4}$$

where k_w (rad/m) is the wave number and l_s (m) is the average stem length in water.

Moreover, in combined current-wave flow, Losada et al. (2016) modified the analytical formulation of Dalrymple et al. (1984):

$$\alpha'=\left[\frac{16}{3\pi}C_D N h_v d\left(\frac{gk_w}{2\sigma_{wc}}\right)^3\frac{\sinh^3 k_w h_v+3\sinh k_w h_v}{3k_w\cosh^3 k_w h}H_0\right]\Big/ \left[g\left(1+\frac{2k_w h}{\sinh 2k_w h}\right)\left(\frac{g}{k_w}\tanh k_w h\right)^{\frac{1}{2}}+ gu\left(3+\frac{4k_w h}{\sinh 2k_w h}\right)+3ku^2\left(\frac{g}{k}\coth k_w h\right)^{\frac{1}{2}}\right], \tag{5}$$

where h_v (m) is the height of vegetation in water; σ_{wc} (rad/s) is the angular frequency associated with combined waves and currents ($\sigma_{wc}=\sigma-u_0 k_w$); σ (rad/s) is angular frequency; u (m/s) is unidirectional current velocity; and g ($\mathrm{m/s}^2$) is the gravitational acceleration.

Overall, different equations for the damping factor (α') can be obtained under different operating conditions, and the researchers all connected α' to the C_D and other easily measurable parameters, such as the water depth, the average stem density, the average stem diameter, and the initial wave height. When spatial wave height is available, the damping factor can be obtained by calibrating the wave attenuation Eq. (1), then C_D can be obtained by the above published equations for α'. Finally, relations between C_D and Reynolds number (Re) and/or Keuglan-Carpenter number (KC) can be obtained by regressions.

3 New expression for predicting the drag coefficient

On one hand, Dean (1979) based on empirical estimates of fluid drag forces acting on vertical and rigid cylinders, the model for the damping of incident wave height (H_0) by coastal plants:

$$K_v=\frac{H}{H_0}=\frac{1}{1+\alpha' X}=\frac{1}{1+\alpha x}=F(x), \tag{6}$$

in which

$$\alpha'=\frac{C_D d}{6\pi h}NH_0 \quad (0\leqslant x=X/L\leqslant 1), \tag{7}$$

where K_v (–) is the scaled wave height; L (m) is the length of vegetation area; α ($=\alpha' L$) (–) is the scaled damping factor; and x (–) is the scaled distance through the vegetation field. $F(x)$ represents a function.

On the other hands, Kobayashi et al. (1993) linearized the horizontal drag force as a function of fluid particle velocity. The local wave height was assumed to decay exponentially with propagation through a vegetation bed according to the following form:

$$\frac{H}{H_0} = \exp\left(-k'X\right) = \exp\left(-kx\right) = G\left(x\right), \tag{8}$$

where k' (m^{-1}) is an exponential damping factor, indicating a slighter decrease in a lower value. k ($=k'L$) (-) is the scaled exponential damping factor, and $G\left(x\right)$ represents another function.

Based on reliable calibration methods, these two expressions are linked. Using the Taylor expansion, when the scaled distance x equals half, the following equations are derived:

$$F\left(x\right) = \frac{2}{\alpha+2} - \frac{4\alpha}{\left(\alpha+2\right)^2}\left(x-\frac{1}{2}\right) + \frac{8\alpha^2}{\left(\alpha+2\right)^3}\left(x-\frac{1}{2}\right)^2 - \frac{16\alpha^3}{\left(\alpha+2\right)^4}\left(x-\frac{1}{2}\right)^3 + R_1\left(x\right), \tag{9}$$

and

$$G\left(x\right) = \frac{1}{\mathrm{e}^{k/2}} - \frac{k}{\mathrm{e}^{k/2}}\left(x-\frac{1}{2}\right) + \frac{k^2}{2\mathrm{e}^{k/2}}\left(x-\frac{1}{2}\right)^2 - \frac{k^3}{6\mathrm{e}^{k/2}}\left(x-\frac{1}{2}\right)^3 + R_2\left(x\right), \tag{10}$$

where $R_1\left(x\right)$ and $R_2\left(x\right)$ are the residual terms. To analyze the importance of each term in Eq. (9), these terms are represented:

$$f_1 = \frac{2}{\alpha+2}, \tag{11}$$

$$f_2 = -\frac{4\alpha}{\left(\alpha+2\right)^2}\left(x-\frac{1}{2}\right), \tag{12}$$

$$f_3 = \frac{8\alpha^2}{\left(\alpha+2\right)^3}\left(x-\frac{1}{2}\right)^2, \tag{13}$$

$$f_4 = -\frac{16\alpha^3}{\left(\alpha+2\right)^4}\left(x-\frac{1}{2}\right)^3. \tag{14}$$

In Eqs (11)–(14), α is larger than zero due to the fact of wave attenuation. Since x is in the range of zero to unit, Eq. (12) can obtain its largest value when x equals zero, and in this case,

$$f_{2,\max} = \frac{2\alpha}{\left(\alpha+2\right)^2}. \tag{15}$$

Similarly, Eq. (13) has the largest value when x equals zero or unit:

$$f_{3,\max} = \frac{2\alpha^2}{\left(\alpha+2\right)^3}. \tag{16}$$

Equation (14) can obtain the largest value in the case of $x=0$:

$$f_{4,\max} = \frac{2\alpha^3}{\left(\alpha+2\right)^4}. \tag{17}$$

To evaluate the relative magnitudes of the different terms of Eq. (9), Fig. 1 presents the factors. The result demonstrates that

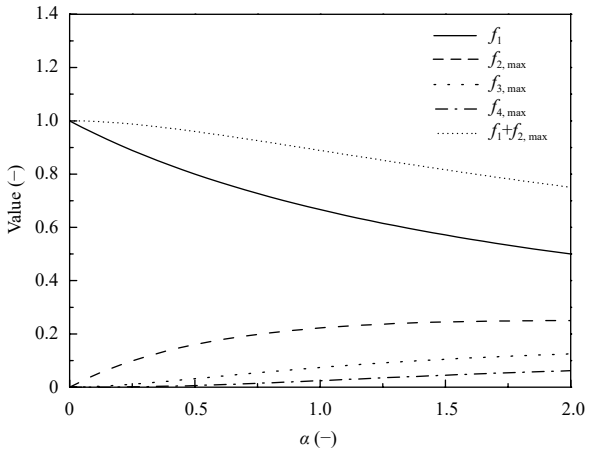

Fig. 1. Comparison between the factors in Eq. (9) as a function of the scaled damping factor α.

the first two terms can play the most significant roles.

Comparably, the importance of each term in Eq. (10) is analyzed and the following expressions are obtained:

$$g_1 = \frac{1}{\mathrm{e}^{k/2}}, \tag{18}$$

$$g_{2,\max} = \frac{k}{\mathrm{e}^{k/2}}, \tag{19}$$

$$g_{3,\max} = \frac{k^2}{8\mathrm{e}^{k/2}}, \tag{20}$$

$$g_{4,\max} = \frac{k^3}{48\mathrm{e}^{k/2}}. \tag{21}$$

Hence, Fig. 2 shows the comparison between these equations as a function of the exponential damping factor. Based on experiences, the value of k is always in the range of zero to two (see for instance, Table 1 in Section 4.2). Under this circumstance, it is obvious that the first two terms are the key ingredients to Eq. (10) and the lower the value of k, which means the slower the wave

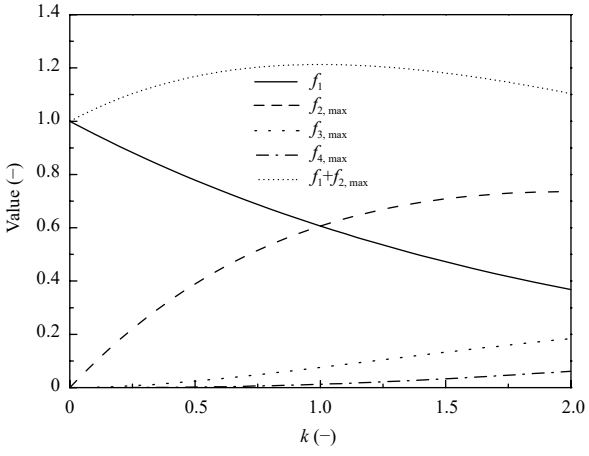

Fig. 2. Comparison between the factors in Eq. (10) as a function of the scaled exponential damping factor k.

attenuate, the more important the first term can be.

Therefore, consider only the first two terms, instead of distance-dependent terms, in Eqs (9) and (10), the proportionality results in:

$$\alpha = \frac{2k}{2-k}. \tag{22}$$

Then, a new expression for the drag coefficient is derived based on Eq. (2):

$$C_D = \frac{12\pi kh}{(2-k)dNH_0L}. \tag{23}$$

Therefore, by measuring local wave height $H(x)$, the exponential damping rate (k) can be calibrated easily, for instance, by Microsoft EXCEL, instead of more professional numerical tools, and C_D can be obtained by Eq. (23).

To look upon Eq. (23) further, a derivative of this equation with respect to k is taken and the result is obtained:

$$(C_D)'_k = \frac{4}{(2-k)^2}\frac{12\pi h}{dNH_0L}. \tag{24}$$

It is obvious that Eq. (24) is larger than zero when k is unequal to 2 since all these parameters are positive. Then C_D is a monotone function of the exponential damping factor. In other word, the more considerably the wave attenuate, the larger the drag coefficient. Besides, the length of the vegetation field is introduced for the bulk drag coefficient comparing to traditional Eq. (2), and it has an inverse correlation with C_D which is reasonable: A wider vegetated area drives a larger (exponential) damping factor and these parameters compensate with each other.

4 Empirical validation

4.1 *Data collection*

To test the new expression Eq. (23) for the bulk drag coefficient, measured data in the published literature has been collected. The researchers in the previous studies showed the values of C_D based on either the calibration method or the direct measurement method.

The laboratory experiments by Hu et al. (2014) were conducted in a wave flume, with a 6 m long vegetation mimic canopy. The mimics were constructed by stiff wooden rods with a height of 0.36 m and a diameter of 0.01 m. Three mimic stem densities (62 stems/m^2, 139 stems/m^2, and 556 stems/m^2) were constructed and control tests with no stems were measured to reduce the effect of friction of flume bed and sidewalls. Meanwhile, two water depths (0.25 m and 0.50 m) were used to study the emergent and submerged conditions. Instantaneous force on stems and horizontal velocity were measured by force transducers and electromagnetic flow manufacture meters. Then the periodic averaged drag coefficient was obtained by the measurements directly.

In addition, Wu et al. (2011) reported a series of experiments in laboratory with a 3.6 m long vegetation field in a sloping beach. The rigid vegetation mimicked by 9.4 mm diameter birch dowels were studied by three stem densities (156 stems/m^2, 350 stems/m^2, and 623 stems/m^2) and two stem heights (0.63 m and 0.48 m). Water surface displacement along the vegetated area were measured by wave gages and video imaging, then the wave height was calculated and the drag coefficient was obtained by fitting the wave attenuation model.

Besides, the laboratory experiments by Wu and Cox (2015) were conducted in a wave flume with a water depth of 12 cm and the 1.8 m long vegetated area was modeled by plastic strips, 5 mm wide by 1 mm thick. The length of the strips was 14 cm and the density was 2 100 stems/m^2. Acoustic wave gages were used to record the free water surface.

Moreover, data in publications by, for instance, Wu and Cox (2016) and Yao et al. (2018), are also collected.

4.2 *Reduction of wave height*

Wave height along the vegetated area is a significant index for the rapid assessment technique, and two examples were taken as Fig. 3 shown. Revisiting the attenuation from Wu and Cox (2015) and Wu et al. (2011), it is clear that Eq. (8) is a reliable relation between the scaled distance and the relative wave height. Results show that the larger the value of k, the faster the wave attenuates. The values of the bulk drag coefficient (C_D) and the calibrated k, besides the data collected from Hu et al. (2014), are listed in Table 1.

Table 1. Values of parameters from references and the calibrated k

Reference	Type of vegetation	Case	Plant height /m	Plant diameter /m	Plant density /(stems·m^{-2})	Incident wave period/s	Incident wave height/m	Collected C_D/(–)	Calibrated k/(–)
Wu et al. (2011)	birch dowels	12436301	0.63	0.009 4	350	1.2	0.085	2.55	0.47
		12435001	0.48	0.009 4	350	1.2	0.084	1.71	0.33
		12636301	0.63	0.009 4	623	1.2	0.083	2.74	0.72
Wu and Cox (2015)	plastic strips	5a	0.12	0.005	2 100	1.6	0.016	2.23	0.43
		5b	0.12	0.005	2 100	1.6	0.024	2.12	0.55
		5c	0.12	0.005	2 100	1.6	0.033	1.95	0.66
		5d	0.12	0.005	2 100	1.6	0.041	1.62	0.76
Wu and Cox (2016)	plastic strips	Case 2	0.12	0.005	1 618	0.6	0.018 7	3.74	0.43
		Case 5	0.12	0.005	1 618	1.2	0.031 3	2.21	0.38
Yao et al. (2018)	PVC pipes	wave 0712	0.20	0.020	139	1.2	0.070	2.68	0.58

4.3 *Comparing the new expression to historical observations*

To validate the new expression for the drag coefficient, a myriad of measured data by previous researchers introduced in Section 4.1 have been collected. The predicted values of the drag coefficient by the new rapid assessment technique are obtained by applying Eq. (23) then. Comparing the outcomes with former published data, the results are displayed in Fig. 4. Based on Hu et al. (2014), which contained a bunch of laboratory studies, operat-

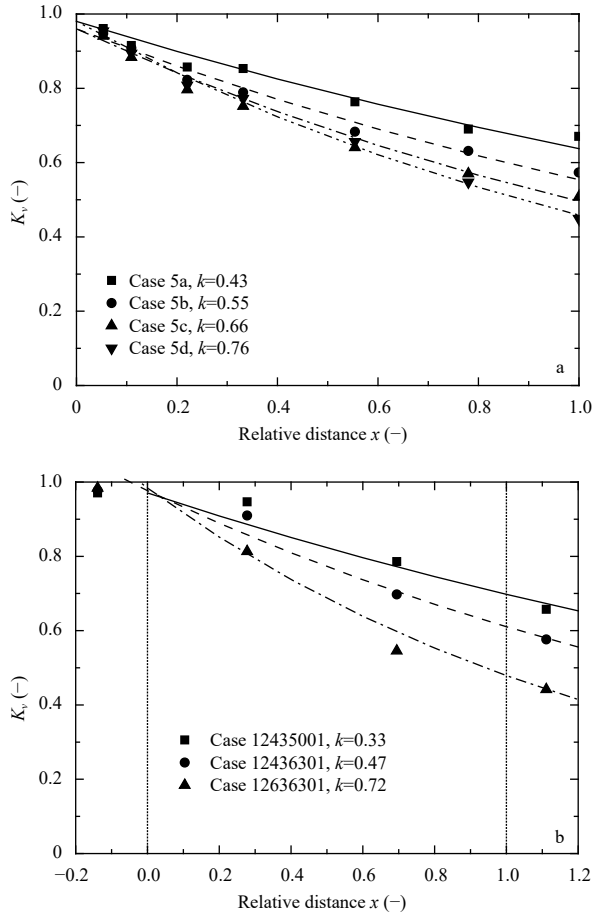

Fig. 3. Wave attenuation for data from Wu and Cox (2015) (a) and Wu et al. (2011) (b). Solid symbols indicate measurements and lines represent the corresponding curves fitted by Eq. (8). Names of cases follow the references.

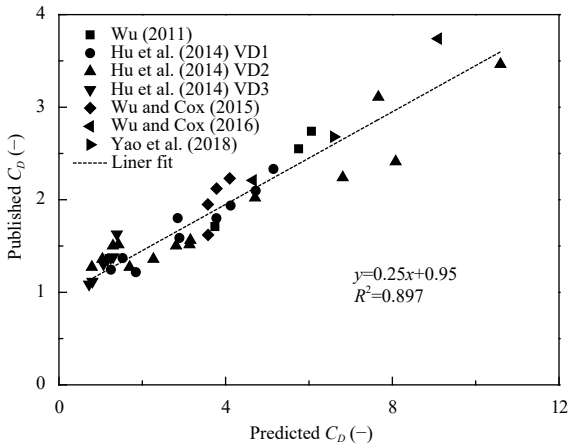

Fig. 4. Comparison of the values of the drag coefficient. The predicted values are obtained by using Eq. (23) and the published data of the drag coefficient are collected from references. Different symbols represent different publications.

ing conditions are represented by VD1, VD2, and VD3 for those three mimic stem densities. The results show that the predicted values are in a range of 0.7 to 10.6 and mostly concentrated on values less than 5.1. More importantly, the predicted values have a strong relation with the 36 historical observations by different researchers. The value of R^2 is 0.90 by regression in Fig. 4, which is quite promising and satisfactory.

The slope of the trendline which equals 0.25 is not troublesome according to Knutson et al. (1982), who has introduced an empirical plant drag coefficient as Eq. (3) shown, with a calibrated value of $C_P = 5$ by minimizing the error between predicted and measured wave heights for data collected in *S. alterniflora* marshes of the Chesapeake Bay. Figure 4 then reveals a predicted equation for the drag coefficient:

$$C_D = \frac{3\pi kh}{(2-k)dNH_0L} + 0.95. \tag{25}$$

In analogical, if Eq. (3) was utilized instead of Eq. (2) in the derivation process above, C_P equals 4 for Eq. (23), which is close to the solution by Knutson et al. (1982).

5 Discussion and conclusions

Wave attenuation by vegetation in wetlands is a large-scale nature-based solution providing different services for humans. To understand wave attenuation, there are two main traditional calibration approaches to the drag effect acting on the vegetation. On one hand, previous researchers found that the decrease of the wave height fits the exponential function well, however, this simple equation has not been applied to the drag coefficient (C_D), one of the most crucial parameters in wave attenuation by vegetation. On the other hand, following the research by Dean (1979), there are several equations based on fitting wave height attenuation for the damping factor α, which is derived as a function of C_D. It is possible that the more complicated the equation, the more precise the equation could be, while it is also necessary to derive a simple approach which can be applicable to different circumstances. By combining these two reliable calibration methods, a simple and visualized relation (Eq. (23)) between the drag coefficient and measurable parameters has been derived. The predicted values yielded from this relation then were compared with a myriad of measured data in the published literature. These 36 published observations come from either the calibration method from the perspective of wave energy dissipation or direct measurement method based on the acting force on the vegetation. Result showed that there is a strong linear relationship between the predicted and published values, and the linear regression revealed a promising R^2 value of 0.90. Moreover, a calibrated value of 4 for the empirical plant drag coefficient C_P introduced by Knutson et al. (1982) has been obtained, which is close to the previous outcome. Finally, a new equation (Eq. (25)) has been obtained for predicting the drag coefficient in wave attenuation by vegetation.

This rapid assessment method for wave attenuation is useful. Firstly, the new method verified that both exponential function and inverse proportional function are reliable and capable for describing the wave attenuation by vegetation satisfactorily, but the new method has built a bridge between them. The exponential damping rate (k'), however, can be obtained much easier than the damping rate (α'), and no professional numerical tools are needed. In addition, it is promising that the new technique can be applied under different circumstances and there is no need to consider which equation should be used for the damping factor (α') by the calibration method. Besides, a bridge between the calibration and direct measurement methods has

been built. Based on different mechanisms, the calibration and direct measurement methods were utilized together to validate the new technique for wave attenuation. The new rapid assessment for the drag coefficient has been validated by a great amount of data under different laboratory conditions, however, the interaction between the vegetation and flow filed is complicated so verification and/or calibration are needed before applying the result to certain cases. Lastly, more data are needed to test the applicability of the new rapid assessment method for the drag coefficient in future studies.

Acknowledgements

We especially thank Zhan Hu for sharing laboratory data.

References

Anderson M E, Smith J M, McKay S K. 2011. Wave dissipation by vegetation. Coastal and Hydraulics Engineering Technical Note ERDC/CHL CHETN-I-82. Vicksburg, MS: US Army Engineer Research and Development Center

Chen Hui, Ni Yan, Li Yulong, et al. 2018. Deriving vegetation drag coefficients in combined wave-current flows by calibration and direct measurement methods. Advances in Water Resources, 122: 217–227, doi: 10.1016/j.advwatres.2018.10.008

Dalrymple R A, Kirby J T, Hwang P A. 1984. Wave diffraction due to areas of energy dissipation. Journal of Waterway, Port, Coastal, and Ocean Engineering, 110(1): 67–79, doi: 10.1061/(ASCE)0733-950X(1984)110:1(67)

Danielsen F, Sørensen M K, Olwig M F, et al. 2005. The Asian tsunami: a protective role for coastal vegetation. Science, 310(5748): 643, doi: 10.1126/science.1118387

Dean R G. 1979. Effects of vegetation on shoreline erosional processes. In: Wetland Functions and Values: The State of Our Understanding. Minneapolis, MN: American Water Resources Association, 415–426

Ghazali N, Zainuddin K, Zainal M Z, et al. 2016. The potential of mangrove forest as a bioshield in Malaysia. In: Proceedings of 2016 IEEE 12th International Colloquium on Signal Processing & Its Applications (CSPA). Malacca City, Malaysia: IEEE, 322–327

Houser C, Trimble S, Morales B. 2015. Influence of blade flexibility on the drag coefficient of aquatic vegetation. Estuaries and Coasts, 38(2): 569–577, doi: 10.1007/s12237-014-9840-3

Hu Zhan, Suzuki T, Zitman T, et al. 2014. Laboratory study on wave dissipation by vegetation in combined current-wave flow. Coastal Engineering, 88: 131–142, doi: 10.1016/j.coastaleng.2014.02.009

Keesstra S, Nunes J, Novara A, et al. 2018. The superior effect of nature based solutions in land management for enhancing ecosystem services. Science of the Total Environment, 610–611: 997–1009, doi: 10.1016/j.scitotenv.2017.08.077

Knutson P L, Brochu R A, Seelig W N, et al. 1982. Wave damping in *Spartina alterniflora* marshes. Wetlands, 2(1): 87–104, doi: 10.1007/BF03160548

Kobayashi N, Raichle A W, Asano T. 1993. Wave attenuation by vegetation. Journal of Waterway, Port, Coastal, and Ocean Engineering, 119(1): 30–48, doi: 10.1061/(ASCE)0733-950X(1993)119:1(30)

Liu Xin, Wang Yebao, Costanza R, et al. 2019. The value of China's coastal wetlands and seawalls for storm protection. Ecosystem Services, 36(3): 100905

Losada I J, Maza M, Lara J L. 2016. A new formulation for vegetation-induced damping under combined waves and currents. Coastal Engineering, 107(1): 1–13

Mazda Y, Magi M, Kogo M, et al. 1997. Mangroves as a coastal protection from waves in the Tong King delta, Vietnam. Mangroves and Salt marshes, 1(2): 127–135, doi: 10.1023/A:1009928003700

Peruzzo P, De Serio F, Defina A, et al. 2018. Wave height attenuation and flow resistance due to emergent or near-emergent vegetation. Water, 10(4): 402, doi: 10.3390/w10040402

Quartel S, Kroon A, Augustinus P G E F, et al. 2007. Wave attenuation in coastal mangroves in the Red River Delta, Vietnam. Journal of Asian Earth Sciences, 29(4): 576–584, doi: 10.1016/j.jseaes.2006.05.008

Reguero B G, Beck M W, Bresch D N, et al. 2018. Comparing the cost effectiveness of nature-based and coastal adaptation: A case study from the Gulf Coast of the United States. PLoS One, 13(4): e0192132, doi: 10.1371/journal.pone.0192132

Schaubroeck T. 2017. Nature-based solutions: sustainable?. Nature, 543(7645): 315

Suzuki T, Hu Z, Kumada K, et al. 2019. Non-hydrostatic modeling of drag, inertia and porous effects in wave propagation over dense vegetation fields. Coastal Engineering, 149: 49–64, doi: 10.1016/j.coastaleng.2019.03.011

Tanaka N, Sasaki Y, Mowjood M I M, et al. 2007. Coastal vegetation structures and their functions in tsunami protection: experience of the recent Indian Ocean tsunami. Landscape and Ecological Engineering, 3(1): 33–45, doi: 10.1007/s11355-006-0013-9

Thampanya U, Vermaat J E, Sinsakul S, et al. 2006. Coastal erosion and mangrove progradation of Southern Thailand. Estuarine, Coastal and Shelf Science, 68(1–2): 75–85, doi: 10.1016/j.ecss.2006.01.011

Wu W C, Cox D T. 2015. Effects of wave steepness and relative water depth on wave attenuation by emergent vegetation. Estuarine, Coastal and Shelf Science, 164: 443–450, doi: 10.1016/j.ecss.2015.08.009

Wu W C, Cox D T. 2016. Effects of vertical variation in vegetation density on wave attenuation. Journal of Waterway, Port, Coastal, and Ocean Engineering, 142(2): 04015020, doi: 10.1061/(ASCE)WW.1943-5460.0000326

Wu W C, Ma G F, Cox D T. 2016. Modeling wave attenuation induced by the vertical density variations of vegetation. Coastal Engineering, 112: 17–27, doi: 10.1016/j.coastaleng.2016.02.004

Wu W M, Ozeren Y, Wren D G, et al. 2011. Phase I Report for SERRI Project No. 80037: Investigation of surge and wave reduction by vegetation. Oxford, United Kingdom: Laboratory Publication

Yanagisawa H, Koshimura S, Miyagi T, et al. 2010. Tsunami damage reduction performance of a mangrove forest in Banda Aceh, Indonesia inferred from field data and a numerical model. Journal of Geophysical Research: Oceans, 115(C6): C06032

Yao Peng, Chen Hui, Huang Bensheng, et al. 2018. Applying a new force–velocity synchronizing algorithm to derive drag coefficients of rigid vegetation in oscillatory flows. Water, 10(7): 906, doi: 10.3390/w10070906